On the Optimal Switching Probability for a Hybrid Cognitive Radio System

Hojin Song, *Student Member, IEEE*, Jun-Pyo Hong, *Student Member, IEEE*, and Wan Choi, *Senior Member, IEEE*

***Abstract*—Cognitive radio (CR) systems are typically classified into two types. In overlay CR, a secondary user opportunistically accesses primary user's spectrum when it is unused, while a secondary user in underlay CR accesses the spectrum at any time as long as the interference power received at a primary user is below a certain level. This paper investigates a hybrid CR system where a secondary user probabilistically changes its spectrum access mode for secondary user's throughput maximization while guaranteeing primary user's target throughput. Basically, the hybrid CR works like overlay CR. The secondary user constantly monitors activity of the primary user and transmits data with maximum transmit power if transmission of the primary user is not detected. However, the only difference from overlay CR is that even when transmission of the primary user is detected, the secondary users are able to access the spectrum with regulated low transmit power with switching rate ϵ. We show that there is a trade-off of increasing ϵ due to recursive interactions between primary and secondary users, and optimizing ϵ is crucial to balance the gain and loss of secondary user's underlay spectrum access. The proposed hybrid CR is shown to achieve higher throughput and be more robust to detection errors than conventional CR systems.**

***Index Terms*—Cognitive radio, overlay, underlay, hybrid, optimal switching probability, throughput maximization.**

I. Introduction

RECENTLY, the demands for wider radio spectrum resources have been dramatically increasing as new various wireless devices have emerged. However, current spectrum allocation policies cause the scarcity of frequency spectra because the spectrum resources are exclusively dedicated to only licensed (primary) users as reported from Federal Communications Commission (FCC) [1]. In order to alleviate the inefficient spectrum utilization, cognitive radio (CR) was proposed in [2] where unlicensed (secondary) users are allowed to access the spectrum licensed to primary users, under certain conditions to protect the quality of service (QoS) of the primary users.

In general, CR techniques are classified into *overlay* CR and *underlay* CR according to the ways of utilizing primary users' spectrum [3]. In overlay CR (also called as *opportunistic spectrum access*), a secondary user monitors the spectrum band to check whether a primary user is transmitting or not, and opportunistically accesses to the spectrum if primary user's transmission is not detected. Accordingly, an accurate detection of primary user's transmission is important for protection of primary user's communications. However, due to shadowing or fading effects [4]–[6], the perfect detection of primary user's transmission is hard in practice so that a primary user cannot be perfectly free from behaviors of a secondary user. There have been several works on protecting QoS of primary users from the detection errors and the interactions between primary and secondary users. In [7], it was shown that there is a tradeoff between sensing performance and secondary user's throughput. The optimal sensing time that maximizes secondary user's throughput while guaranteeing a certain level of detection probability was analyzed. The concept of queueing process is applied to CR in [8], [9] to rather exploit the interaction between primary and secondary users. Recently, [10] derived multiuser diversity gain which can be obtained from opportunistic secondary user scheduling.

In underlay CR (also called as *spectrum sharing*), a secondary user is allowed to access spectrum at any time as long as the received interference at a primary user is regulated below a predetermined level, i.e., *interference temperature* [11]. Interference temperature represents the tolerable interference level at a primary user caused by the activity of a secondary user. Since a secondary user in underlay CR systems can always access the licensed spectrum by regulating transmit power not to cause harmful interference to a primary user, the underlay CR system is regarded as a more aggressive spectrum access technique compared to the overlay CR system. One of the most representative applications of the underlay CR is ultra-wideband (UWB) [12]. Based on the attractive concept of underlay CR, there are many studies on underlay CR. In [13], ergodic capacity of a secondary user with an instantaneous/average interference power constraint was analyzed in various fading channels. In [14], ergodic and outage capacities under an instantaneous/average interference power constraint and under an instantaneous/average transmit power constraint were derived. For multiple secondary users, multiuser diversity in underlay CR was investigated in [15] and capacity scaling law of multiple-access and broadcast channels was studied in [16]. Also, cooperative diversity in underlay CR systems was discussed in [17].

In order to exploit advantages of both underlay and overlay CR systems, the combined CR approaches have recently been proposed in [18]–[22]. The combined approaches are called by various names, such as hybrid CR [18], [19], sensing based spectrum sharing [20], [21], and mixed access for spectrum sharing [22]. For convenience, we call all of the combined approaches as hybrid CR. There are many specific ways of exploiting the advantages. In [18], [19], a secondary user transmits information bits over unused spectrum bands with

Manuscript received March 3, 2012; revised September 4 and November 28, 2012; accepted January 13, 2013. The associate editor coordinating the review of this manuscript and approving it for publication was X. Ma.

This work was supported by the National Research Foundation of Korea(NRF) grant funded by the Korea government(MEST) (No. 2012-047720).

The authors are with Department of Electrical Engineering, Korea Advanced Institute of Science and Technology (KAIST), Daejeon, 305-701, Korea (e-mail: {hojinsong, jp_hong}@kaist.ac.kr, wchoi@ee.kaist.ac.kr).

Digital Object Identifier 10.1109/TWC.2013.022213.120311

overlay mode and redundant parity check bits over under-used spectrum bands with underlay mode. However, the analysis and design of those papers did not take into account sensing errors and the interference power constraint of underlay mode. In [20]–[22], the secondary network in hybrid CR constantly monitors activity of the primary user. When transmission of the primary user is not detected, the secondary user opportunistically transmits its data with relatively high transmit power as like the overlay CR. Otherwise, the secondary user transmits its data with regulated low power as like underlay CR. These papers [20]–[22] proposed suboptimal and optimal power allocation algorithms for maximizing secondary user's throughput and showed that the hybrid CR system always outperforms the conventional CR system.

Although the initial works on hybrid CR have successfully motivated the combination between two different CR approaches, analysis and system design in those works discarded mutual interference or decoupled primary and secondary networks by neglecting recursive interactions. For example, interference from a secondary user to a primary user caused by sensing errors or underlay transmission could degrade primary user's performance so that the primary user might try to compensate for the degradation by increasing transmit power or retransmission to satisfy a predetermined QoS level. Then, those reactions of the primary user again affect secondary users' communications, but these recursive interactions are totally neglected in the previous works on hybrid CR. If those recursive interactions are taken into account, the conclusion of the previous works that a hybrid CR system always outperforms the conventional CR systems could be modified. Specifically, if the recursive interactions are considered, the idle probability of a primary user in a hybrid CR system will be lower than that of a conventional overlay CR system because a primary user should more frequently access its spectrum to make up the degradation caused by the secondary user. The lower idle probability of a primary user results in the higher probability that secondary users communications are interfered with a primary user. Consequently, in some environments, a hybrid CR system could have lower throughput than a conventional overlay CR system even though a hybrid CR system increases total transmission time of a secondary user.

In this context, this paper proposes a hybrid CR system based on probabilistic switching and investigates the performance of the proposed hybrid CR system when the recursive interactions between primary and secondary users are taken into account. In the proposed hybrid CR system, the spectrum access of a secondary user by underlay CR mode is probabilistically determined for balancing gain and loss of secondary user's spectrum access by underlay mode. We optimize the mode switching rate and show that the hybrid CR system with the optimal switching rate significantly improves the performance of the conventional CR systems. It is also shown that the proposed hybrid CR is more robust to detection error than the conventional CR system.

The rest of this paper is organized as follows. In section II, channel and traffic models are described. In section III and IV, conventional overlay, underlay, and hybrid CR systems are described and analyzed, respectively. For the multiuser scenarios, we extend our work to the secondary multiple access channel in section V. Section VI compares throughput of a secondary user in the hybrid CR system with those in conventional overlay and underlay CR systems. Finally, we draw conclusions in section VII.

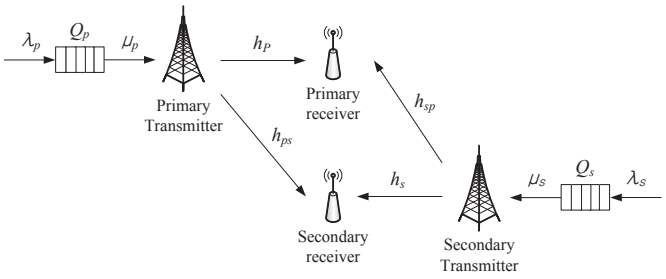

Fig. 1. System and traffic model.

II. Channel and Traffic Model

A. Channel Model

Fig. 1 depicts our CR system configuration consisting of a primary user pair and a secondary user pair. The channel gains from the primary transmitter to the primary receiver and from the secondary transmitter to the secondary receiver are denoted by h_{pp} and h_{ss}, respectively. Similarly, h_{sp} and h_{ps} are the interference channel gains from the secondary transmitter to the primary receiver and from the primary transmitter to the secondary receiver, respectively. We assume that all the channels suffer from independent Rayleigh flat fading, and each channel power gain has mean $\mathbb{E}\left[|h_{ij}|^2\right] = 1/\beta_{ij}$, for $i, j \in \{p, s\}$. β_{ij} reflects the effect of large-scale fading and can be thought as a distance between transmitter and receiver. Hence, as β_{ij} decreases (i.e., transmitter and receiver are getting closer), the average channel power gain increases. It is assumed that the channels are static during each time slot. The additive noise at each receiver is an independent identically distributed (i.i.d.) circularly symmetric complex Gaussian random variable with zero mean and variance σ^2. We assume that the primary and secondary transmitters do not have channel state information unless otherwise stated.

B. Traffic Model

We assume *packet-by-packet* transmission as in [9] so that the spectrum is accessed in a time-slotted manner. In other words, each primary and secondary transmitter can transmit at most one packet per each time slot. The incoming packet traffic at the primary transmitter is modeled by *Bernoulli* process with average arrival rate λ_p. For analytical tractability, we assume the primary and secondary transmitters are equipped with infinite-length buffers to store the incoming packets. The secondary user is assumed to have a heavy traffic; if the packet generation rate of the secondary user is high, the secondary user always has at least one packet in its queue with high probability. This assumption enables tractable analysis by decoupling the secondary queueing condition from the primary queueing process and is well justified in practice because the service rate of the secondary user is generally

lower than its packet generation rate owing to the secondary user's unfavorable communication conditions.

The average packet departure rate μ_i ($i \in \{p, s\}$) is interpreted as the probability of successful packet transmission during a time slot, and is directly translated into average throughput which is related to outage probability in non-ergodic channels. For a target rate of the primary user R_p [bits/sec/Hz], the outage probability is represented by

$$P_{p,\text{out}} = \Pr\left[\log\left(1+\frac{|h_{pp}|^2 P_p}{\sigma^2+|h_{sp}|^2 P_s}\right) < R_p\right] = \Pr\left[\frac{|h_{pp}|^2 P_p}{\sigma^2+|h_{sp}|^2 P_s} < a_p\right], \quad (1)$$

where P_p and P_s are the power transmitted by primary and secondary transmitters, respectively, and $a_p = 2^{R_p} - 1$. The equation (1) indicates the average departure rate of the primary user is represented by $\mu_p = 1 - P_{p,\text{out}}$. Then, the average throughput is given in terms of departure rate or outage probability by

$$T_p = R_p \mu_p = R_p(1 - P_{p,\text{out}}). \quad (2)$$

The outage probability $P_{s,\text{out}}$, average departure rate μ_s, and average throughput of the secondary user T_s have the similar relationship to those of the primary user.

As a QoS constraint of the primary user, the departure rate of the primary user should be guaranteed to be greater than a target threshold μ_{th} so that the secondary user should carefully control the interference to the primary user. The constraint is written by $\mu_p \geq \mu_{th}$. The threshold μ_{th} should be selected to make primary user's system stable such that $\mu_{p,max} > \mu_{th} > \lambda_p$ [24], where $\mu_{p,max}$ represents the average departure rate of primary user without any interference from the secondary user such that

$$\mu_{p,max} = \Pr\left[\frac{|h_{pp}|^2 P_p}{\sigma^2} \geq a_p\right] = \exp\left(-\frac{\beta_{pp} a_p \sigma^2}{P_p}\right). \quad (3)$$

Hereafter, we simply refer to "average packet departure rate" as "departure rate", "average packet arrival rate" as "arrival rate", and "average throughput" as "throughput", respectively.

The arrival and departure rates of the primary user are closely related to the probability of primary user's transmission. According to queueing theory [25], the probability that the primary user's queue has at least one packet to transmit, or the probability that the primary user transmits a packet, can be represented by $\frac{\lambda_p}{\mu_p}$. Accordingly, growing λ_p and diminishing μ_p result in frequent transmissions of the primary user.

III. Conventional Approaches in CR System

In this section, we discuss the conventional overlay and underlay CR approaches. In each subsection, the difference between overlay CR and underlay CR will be shown, and throughput of a primary user T_p and throughput of a secondary user T_s in each approach are derived, respectively.

A. Overlay CR System

In overlay CR, a secondary user senses the activity of a primary user at the beginning of each time slot. Only if a primary user is detected as an idle state, the secondary user transmits its packet. Thus the system performance depends on sensing errors which are typically captured by miss detection probability p_m and false alarm probability p_f. The miss detection probability p_m is the probability that the secondary user considers the spectrum unused even though it is already occupied by the primary user. Hence, the secondary user accesses the spectrum due to the missed detection of the primary user and causes interference to the primary receiver. The false alarm probability p_f is the probability that the secondary user declares primary user is active even though the primary user is idle. Thus, the secondary user misses an opportunity to access the spectrum due to the false alarm. The spectrum sensing performance (i.e., p_f and p_m) is affected by several factors. In other words, the sensing performance is determined by sensing rule with some parameters such that primary service power, packet generation rate, and channel power gain. To take into account of interactions between the sensing parameter (i.e., the primary user's transmit power) and throughput of the secondary user, we adopt the energy detector which is one of the most common spectrum sensing techniques.

The departure rate of the primary user in overlay CR μ_p^{over} can be represented as

$$\mu_p^{over} = \mu_{p,max} D^{over}, \quad (4)$$

where $D^{over} = 1 - p_m + \frac{p_m \beta_{sp} P_p}{\beta_{sp} P_p + \beta_{pp} a_p P_s^{over}}$ corresponds to a loss factor of μ_p^{over} caused by p_m. This is because when $p_m = 0$, the departure rate μ_p^{over} equals to $\mu_{p,max}$ which is the departure rate of primary user without any interference from the secondary user. A derivation of μ_p^{over} is in Appendix A. Then, The throughput of the primary user is represented by $T_p^{over} = R_p \mu_p^{over}$.

The secondary transmit power P_s^{over} should satisfy two constraints: the primary QoS constraint and the maximum transmit power constraint. According to the QoS constraint $\mu_p^{over} \geq \mu_{th}$, the maximum allowable transmit power is represented by

$$P_{s,\mu}^{over} = \begin{cases} \infty, & \text{if } (1-p_m)\exp(-\frac{\beta_{pp} a_p \sigma^2}{P_p}) > \mu_{th} \\ \frac{\beta_{sp} P_p}{\beta_{pp} a_p}\left(\frac{p_m}{\mu_{th}\exp(\frac{\beta_{pp} a_p \sigma^2}{P_p}) + p_m - 1} - 1\right), & \\ \text{if } (1-p_m)\exp(-\frac{\beta_{pp} a_p \sigma^2}{P_p}) \leq \mu_{th} & \end{cases}. \quad (5)$$

Because the actual transmit power should not exceed the maximum transmit power constraint, $P_{s,\mu}^{over}$ is clipped by $P_{s,max}$ if $P_{s,\mu}^{over} > P_{s,max}$.

$$P_s^{over} = \begin{cases} P_{s,max}, & \text{if } P_{s,max} \leq P_{s,\mu}^{over} \\ P_{s,\mu}^{over}, & \text{if } P_{s,max} > P_{s,\mu}^{over} \end{cases}. \quad (6)$$

The departure rate of the secondary user in the overlay CR μ_s^{over} can be represented as

$$\mu_s^{over} = \left(1 - \frac{\lambda_p}{\mu_p^{over}}\right)(1-p_f)\mu_{s,idle}^{over} + \frac{\lambda_p}{\mu_p^{over}} p_m \mu_{s,active}^{over}, \quad (7)$$

where $\mu_{s,idle}^{over}$ and $\mu_{s,active}^{over}$ are defined in Appendix B. Also a detailed derivation of μ_s^{over} is in Appendix B. Accordingly, the throughput of the secondary user in overlay CR is represented by $T_s^{over} = R_s \mu_s^{over}$.

B. Underlay CR System

In underlay CR system, a secondary user does not need to sense the activity of a primary user. It transmits its packet at any time even though the primary user occupies the spectrum. But the power transmitted by the secondary transmitter must be carefully controlled to keep the interference to the primary user below an interference temperature. We assume that the secondary transmitter has the channel information of the interfering link to the primary receiver. Based on the interference channel information h_{sp}, the secondary transmitter can adapt its transmit power to the instantaneous interference channel condition. The information of h_{sp} can be obtained by feedback from the primary receiver directly, or by a system manager indirectly.

In underlay CR, the transmit power of the secondary user having information of h_{sp} is denoted by P_s^{under}. The P_s^{under} should be determined to satisfy the QoS constraint of the primary user such that

$$\mu_p^{under}(|h_{sp}|^2) = \Pr\left[\frac{|h_{pp}|^2 P_p}{\sigma^2 + |h_{sp}|^2 P_s^{under}} > a_p \Big| |h_{sp}|^2 = x\right] \geq \mu_{th}. \quad (8)$$

Then, since $|h_{pp}|^2$ follows the exponential distribution, the maximum allowable power to guarantee the QoS constraint $P_{s,\mu}^{under}$ can be represented by

$$P_{s,\mu}^{under} = \frac{1}{|h_{sp}|^2}\left[\frac{-P_p \ln \mu_{th}}{\beta_{pp} a_p} - \sigma^2\right] = \frac{Q}{|h_{sp}|^2}, \quad (9)$$

where $Q = \frac{-P_p \ln \mu_{th}}{\beta_{pp} a_p} - \sigma^2$ denotes an interference temperature. Based on (9), the actual transmit power of the secondary user P_s^{under} is determined as

$$P_s^{under} = \begin{cases} P_{s,max} & \text{if } |h_{sp}|^2 P_{s,max} \leq Q \\ P_{s,\mu}^{under} = \frac{Q}{|h_{sp}|^2} & \text{if } |h_{sp}|^2 P_{s,max} > Q \end{cases}. \quad (10)$$

Thus, the departure rate of the primary user μ_p^{under} can be rewritten by

$$\mu_p^{under} = \mu_{p,max} D^{under}, \quad (11)$$

where $D^{under} = \frac{\frac{\beta_{sp} P_p}{P_{s,max}} + \exp\left(\frac{-(\beta_{pp} a_p P_{s,max} + \beta_{sp} P_p) Q}{P_p P_{s,max}}\right) \beta_{pp} a_p}{\frac{\beta_{sp} P_p}{P_{s,max}} + \beta_{pp} a_p}$ denotes a loss factor in departure rate caused by the QoS constraint. μ_p^{under} is derived in Appendix C. Throughput of the primary user is represented by $T_p^{under} = R_p \mu_p^{under}$.

The departure rate of secondary user μ_s^{under} is written by

$$\mu_s^{under} = \left(1 - \frac{\lambda_p}{\mu_p^{under}}\right) \mu_{s,idle}^{under} + \frac{\lambda_p}{\mu_p^{under}} \mu_{s,active}^{under}, \quad (12)$$

where $\mu_{s,idle}^{under}$ and $\mu_{s,active}^{under}$ are defined in Appendix D, respectively. Also, a detailed derivation of μ_s^{under} is in Appendix D. The throughput of the secondary user in underlay CR is represented by $T_s^{under} = R_s \mu_s^{under}$.

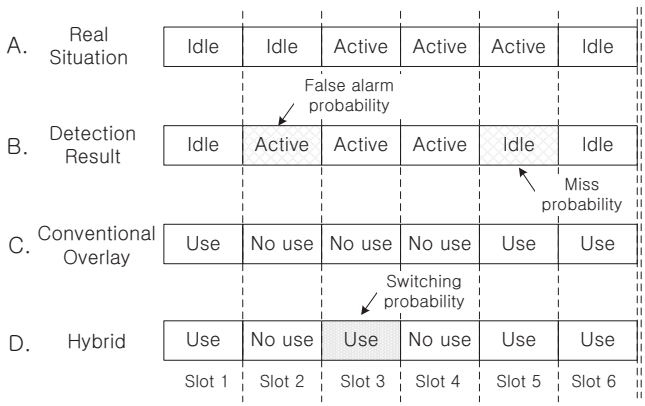

Fig. 2. Example of the conventional overlay CR system and the hybrid CR system in time-slotted manner.

Finally, if the secondary user does not have the channel information of the interfering link to the primary user, it cannot adapt transmit power to the instantaneous interference channel condition. This case is dealt with in Appendix E.

IV. Hybrid Strategy in CR System

In this section, we describe a *hybrid strategy* in a CR system. Although both of overlay and underlay approaches are fundamentally the same from the perspective that the secondary users communicate while guaranteeing QoS of the primary users, they have a big difference in the way of reusing the spectrum. In order to guarantee QoS of the primary users, the secondary users in the overlay CR are allowed to access the spectrum only when the transmission of the primary users is not detected in the secondary network. On the other hand, the secondary users in the underlay CR access the spectrum with low transmit power in order to prevent the primary user from QoS degradation. Consequently, the overlay CR has an advantage over underlay CR in transmit power, and the underlay CR has an advantage over overlay CR in spectrum accessing time. If the target QoS of the primary user can be satisfied in the presence of secondary user's transmission, the evacuation of the secondary user in an overlay CR system is unnecessary and can hurt efficiency of spectrum utilization. This reasoning naturally motivates a new strategy that combines overlay and underlay CR modes in order to exploit advantages of both CR approaches.

In the conventional overlay CR system, if the secondary user detects primary user's transmission, it does not accesses the spectrum. But in the hybrid CR system, even though the secondary user detects primary user's transmission, it accesses the spectrum in underlay CR mode with a mode switching rate ϵ to increase its throughput [22], [23]. As illustrated in Fig 2, the secondary user with conventional overlay CR does not access the spectrum when it detects that the primary user uses the spectrum. However, in time slot 3, the secondary user with hybrid CR accesses the spectrum with switching probability ϵ even though the primary user is detected as active.

The switching rate ϵ is determined for maximizing the throughput of the secondary user while satisfying QoS requirement for the primary user. Note that $\epsilon = 0$ corresponds to the conventional overlay CR system. We derive the optimal switching rate ϵ_{opt} through mathematical analysis. With the

optimized value ϵ_{opt}, it is shown that the hybrid CR system outperforms the conventional overlay CR system.

In the hybrid CR system where the secondary user knows the interference channel information, the departure rate of the primary user is represented by

$$\begin{aligned}\mu_p^{hybrid}(\epsilon) &= p_m \Pr\left[\frac{|h_{pp}|^2 P_p}{\sigma^2 + |h_{sp}|^2 P_s^{over}} \geq a_p\right] \\ &\quad + (1-\epsilon)(1-p_m)\Pr\left[\frac{|h_{pp}|^2 P_p}{\sigma^2} \geq a_p\right] \\ &\quad + \epsilon(1-p_m)\Pr\left[\frac{|h_{pp}|^2 P_p}{\sigma^2 + |h_{sp}|^2 P_s^{under}} \geq a_p\right] \\ &= \mu_{p,max}\left(D^{over} - \epsilon(1-p_m)\left(1 - D^{under}\right)\right). \end{aligned} \tag{13}$$

If the secondary user does not have the channel information of the interfering link, the departure rate of the primary user in the hybrid CR is represented as (13) by substituting P_s^{under} and D^{under} with $\bar{P}_s^{under}$ and $\bar{D}^{under}$, respectively. The closed expressions of $\bar{P}_s^{under}$ and $\bar{D}^{under}$ are derived in Appendix E. As shown in the first equality of (13), the departure rate $\mu_p^{hybrid}(\epsilon)$ is a function of ϵ and is composed of three terms. The first and the second terms represent the departure rate when the secondary user accesses the spectrum in overlay CR mode, and the third term represents the departure rate when the secondary user transmits its packet in underlay CR mode with a switching probability ϵ. The throughput of the primary user in the hybrid CR is represented by

$$T_p^{hybrid}(\epsilon) = R_p \mu_p^{hybrid}(\epsilon). \tag{14}$$

A. Primary QoS Constraint

Unlike the conventional overlay CR, there is additional interference at the primary receiver in the hybrid CR system because the secondary user sometimes accesses the spectrum in underlay CR mode even if primary user's transmission is detected. As a QoS constraint of the primary user, the departure rate of the primary user should be guaranteed to be greater than a target threshold departure rate μ_{th}, i.e.,

$$\mu_p^{hybrid}(\epsilon) \geq \mu_{th}. \tag{15}$$

From (15), the switching rate ϵ is upper bounded as

$$\epsilon \leq \min\left(\frac{D^{over} - \frac{\mu_{th}}{\mu_{p,max}}}{(1-p_m)\left(1 - D^{under}\right)}, 1\right) = \epsilon_{max}, \tag{16}$$

where ϵ_{max} denotes the maximum allowable value of the switching rate ϵ to guarantee the QoS of the primary user. The QoS constraint of the primary user μ_{th} is assumed to be less than the achievable departure rate of a primary user in a conventional overlay CR system $\mu_p^{hybrid}(0)$, i. e., $\mu_{th} \leq \mu_p^{hybrid}(0) = \mu_p^{over}$. If the constraint μ_{th} is set to be μ_p^{over}, the maximum switching rate ϵ_{max} becomes 0 so that the hybrid CR system should operate in overlay CR mode only to satisfy primary user's QoS constraint.

B. Optimization of Switching Rate

In previous subsection, we showed the maximum allowable switching rate ϵ_{max} to guarantee primary user's QoS constraint. However, the maximum allowable switching rate ϵ_{max} may not be the optimal value of ϵ maximizing secondary user's throughput because there is a *trade-off* in increasing the switching rate ϵ; the spectrum access time in underlay CR mode increases with ϵ but the increased interference in underlay CR mode reduces primary user's departure rate $\mu_p^{hybrid}(\epsilon)$, and hence opportunities of secondary user's spectrum access without interference from the primary user decrease with ϵ due to the decreased idle probability of the primary user given by $1 - \frac{\lambda_p}{\mu_p^{hybrid}(\epsilon)}$. Therefore, the switching rate ϵ should be optimized for maximizing secondary user's throughput while satisfying primary user's QoS constraint.

In the hybrid CR system, secondary user's departure rate when the interference channel information is known at the secondary transmitter, is obtained by

$$\begin{aligned}&\mu_s^{hybrid}(\epsilon) \\ &= \left(1 - \frac{\lambda_p}{\mu_p^{hybrid}(\epsilon)}\right)\left((1-p_f)\mu_{s,idle}^{over} + \epsilon p_f \mu_{s,idle}^{under}\right) \\ &\quad + \frac{\lambda_p}{\mu_p^{hybrid}(\epsilon)}\left(p_m \mu_{s,active}^{over} + \epsilon\left(1-p_m\right)\mu_{s,active}^{under}\right) \\ &= (1-p_f)\mu_{s,idle}^{over} + \epsilon p_f \mu_{s,idle}^{under} \\ &\quad + \frac{\lambda_p}{\mu_p^{hybrid}(\epsilon)}\left(p_m \mu_{s,active}^{over} - (1-p_f)\mu_{s,idle}^{over}\right) \\ &\quad + \epsilon\frac{\lambda_p}{\mu_p^{hybrid}(\epsilon)}\left((1-p_m)\mu_{s,active}^{under} - p_f \mu_{s,idle}^{under}\right). \end{aligned} \tag{17}$$

If the secondary transmitter does not know the interference channel information, secondary user's departure rate is represented as (17) by substituting $\mu_{s,active}^{under}$ and $\mu_{s,idle}^{under}$ with $\bar{\mu}_{s,active}^{under}$ and $\bar{\mu}_{s,idle}^{under}$, respectively. The closed expressions of $\bar{\mu}_{s,active}^{under}$ and $\bar{\mu}_{s,idle}^{under}$ are derived in Appendix E. Using (17), we can formulate an optimization problem to find the optimal value of ϵ as

$$\begin{aligned}\max_{0\leq\epsilon\leq\epsilon_{max}}\Bigg(&\epsilon p_f \mu_{s,idle}^{under} + \frac{\lambda_p}{\mu_p^{hybrid}(\epsilon)}\Big(p_m \mu_{s,active}^{over} - (1-p_f)\mu_{s,idle}^{over} \\ &+ \epsilon\left((1-p_m)\mu_{s,active}^{under} - p_f \mu_{s,idle}^{under}\right)\Big)\Bigg). \end{aligned} \tag{18}$$

For simple notations, we define A, B, C, D, E as follows:

$$A = p_f \mu_{s,idle}^{under}, \tag{19}$$

$$B = \lambda_p\left(p_m \mu_{s,active}^{over} - (1-p_f)\mu_{s,idle}^{over}\right), \tag{20}$$

$$C = \lambda_p\left((1-p_m)\mu_{s,active}^{under} - p_f \mu_{s,idle}^{under}\right), \tag{21}$$

$$D = \mu_{p,max} D^{over}, \tag{22}$$

$$E = \mu_{p,max}(1-p_m)\left(1 - D^{under}\right). \tag{23}$$

Then, the optimization problem in (18) can be rewritten by

$$\max_{0\leq\epsilon\leq\epsilon_{max}} f(\epsilon), \tag{24}$$

where $f(\epsilon) = A\epsilon + \frac{B+C\epsilon}{D-E\epsilon} = A\epsilon - \frac{C}{E} - \frac{1}{E^2}\frac{BE+CD}{\epsilon - \frac{D}{E}}$.

According to the relationship between B, C, D, E, we classify $f(\epsilon)$ into two cases and analyze the optimal value of ϵ for each case.

1) Case 1 : $BE + DC \geq 0$

Since A is a non-negative value and $\frac{D}{E} > 1$, $f(\epsilon)$ is a monotonic increasing function of ϵ if $BE + DC$ is greater than 0. Thus, the optimal value of ϵ in the case is

$$\epsilon_{opt} = \epsilon_{max}. \tag{25}$$

2) Case 2 : $BE + DC < 0$

The first and the second derivatives of the objective function are given, respectively, by

$$f'(\epsilon) = A + \frac{\frac{D}{E}\left(\frac{B}{D} + \frac{C}{E}\right)}{(\epsilon - \frac{D}{E})^2}, \tag{26}$$

$$f''(\epsilon) = -\frac{\frac{D}{E}\left(\frac{B}{D} + \frac{C}{E}\right)}{(\epsilon - \frac{D}{E})^3}. \tag{27}$$

Since $\frac{D}{E}$ is always greater than 1, $f''(\epsilon)$ always has a negative value for all possible values of ϵ (i.e., $0 \leq \epsilon \leq \epsilon_{max} \leq 1 < \frac{D}{E}$). Then, $f(\epsilon)$ is a concave function of ϵ, and the value ϵ^* that makes $f'(\epsilon^*)$ equal to 0 maximizes the objective function $f(\epsilon)$. From (26), the value ϵ^* can be obtained by

$$\epsilon^* = \frac{D}{E} - \sqrt{-\frac{\frac{D}{E}\left(\frac{B}{D} + \frac{C}{E}\right)}{A}}. \tag{28}$$

Consequently, the optimal value of ϵ can be obtained by

$$\epsilon_{opt} = \begin{cases} 0 & \text{if } \epsilon^* < 0 \\ \epsilon^* & \text{if } 0 \leq \epsilon^* \leq \epsilon_{max} \\ \epsilon_{max} & \text{if } \epsilon^* > \epsilon_{max} \end{cases}. \tag{29}$$

Therefore, the throughput of the secondary user in hybrid CR with the optimal switching rate is represented by

$$T_s^{hybrid}(\epsilon_{opt}) = R_s \mu_s^{hybrid}(\epsilon_{opt}). \tag{30}$$

V. Extension to Multiple Secondary Users

In this section, we extend our results to a network consisting of a primary transmitter/receiver pair, a secondary receiver, and N secondary transmitters trying to communicate with a common secondary receiver. To minimize interference to the primary receiver, a secondary user who has the lowest interference channel power gain is scheduled for transmission as follows:

$$\hat{i} = \underset{1 \leq i \leq N}{\arg\min} \ |h_{sp,i}|^2, \tag{31}$$

where $h_{sp,i}$ denotes a channel gain of the link from the ith secondary transmitter to the primary receiver. Once a secondary user has been selected for transmission, the effective network consists of a single primary transmitter/receiver pair, a secondary receiver, and the selected secondary transmitter. Since each channel power gain $|h_{sp,i}|^2$ is independent exponential random variable with mean $\mathbb{E}\left[|h_{sp,i}|^2\right] = 1/\beta_{sp,i}$, the channel power gain of the link from the selected secondary transmitter to the primary receiver $|h_{sp,\hat{i}}|^2$ follows an exponential random variable with the parameter $\sum_{i=1}^{N} \beta_{sp,i}$. In the analysis of the throughput, the only change from the single secondary user case to the multi-secondary user case is the distribution of the interfering channel power gain. Eventually, the analysis results in the multiuser case can be obtained by replacing β_{sp} in section III and IV with $\sum_{i=1}^{N} \beta_{sp,i}$.

Corollary 1: In the secondary multiple access channel with a large number of secondary transmitters, the optimal switching rate is equal to 1 and the secondary throughput of the hybrid CR is the same as that of the conventional underlay CR with opportunistically selected secondary user.

Proof: The proof of corollary 1 is in Appendix F. ■

VI. Simulation Results

In our simulation results, we consider an energy detector as a spectrum sensing rule for the secondary user. Using the energy detector [6], the missed detection probability p_m and the false alarm probability p_f are given, respectively, by

$$p_m = \left(\exp\left(-\frac{\tau}{2(1+\bar{\gamma})}\right) - \exp(-\frac{\tau}{2}) \sum_{k=0}^{m-2} \frac{(\tau\bar{\gamma})^k}{k! 2^k (1+\bar{\gamma})^k}\right) \times \left(\frac{1+\bar{\gamma}}{\bar{\gamma}}\right)^{m-1} + 1 - \sum_{k=0}^{m-2} \frac{\exp\left(-\frac{\tau}{2}\right)\left(\frac{\tau}{2}\right)^k}{k!}, \tag{32}$$

$$p_f = \frac{\Gamma(m, \tau/2)}{\Gamma(m)}, \tag{33}$$

where τ is a detection threshold, m is a product of signal bandwidth and a detection time interval, and $\bar{\gamma}$ denotes average SNR given by $\bar{\gamma} = \frac{P_p}{\beta\sigma^2}$, where $\frac{1}{\beta}$ denotes average channel power gain between the primary transmitter and the secondary transmitter. $\Gamma(\cdot)$ and $\Gamma(\cdot,\cdot)$ are complete and incomplete gamma functions, respectively. From (32) and (33), we can notice that p_m depends on the primary transmission power, average channel power gain β, whereas p_f does not. The performance of the energy detector can be characterized by receiver operating characteristics (ROC) curve, which plots achievable pairs of $(1 - p_m, p_f)$. For other sensing techniques [4]–[7], we can substitute the equations of p_m and p_f in (32) and (33) with those of the considered sensing technique or proper values of operation point on the ROC curve.

Fig. 3 shows the ROC curves of the energy detector for several values of average SNR $\frac{P_p}{\beta\sigma^2}$. The product of the bandwidth and the detection time, m is assumed to be 5. It is confirmed that the sensing performance of energy detector is improved as the SNR increases. By changing the value of the detection threshold τ, we can obtain any point in the ROC curve. The point A, B, and C in Fig. 3 represent operation points when τ =14, 15, and 16, respectively.

Fig. 4 shows average throughputs of the secondary user in the conventional overlay and hybrid CR systems versus the switching rate ϵ for different operation points in Fig. 3. System parameters are chosen as follow: $\frac{P_p}{\sigma^2} = \frac{P_{s,max}}{\sigma^2}$ = 16 [dB], λ_p = 0.4 [packets/sec], u_{th} = 0.6 [packets/sec], $R_p = \log(a_p + 1)$ = 2 [bits/sec/Hz], $R_s = \log(a_s + 1)$ = 1 [bits/sec/Hz], and large scaling fading factor $\beta_{pp} = \beta_{ps} = \beta_{sp} = \beta_{ss} = \beta = 1$. In this environment, $\frac{Q}{\sigma^2}$ = 7.6184 [dB], μ_p^{under} = 0.6211 [packets/sec], D^{under} = 0.6697 are fixed values, and the optimal switching rates ϵ_{opt} are determined by 0.6198, 0.4097, and 0.1438 for point A, B and C, respectively. According to the value of ϵ, the hybrid scheme could be equivalent to overlay CR scheme ($\epsilon = 0$) or the conventional hybrid CR scheme ($\epsilon = 1$) [20], [21]. It is confirmed that the secondary throughput of the hybrid CR scheme with ϵ_{opt} is

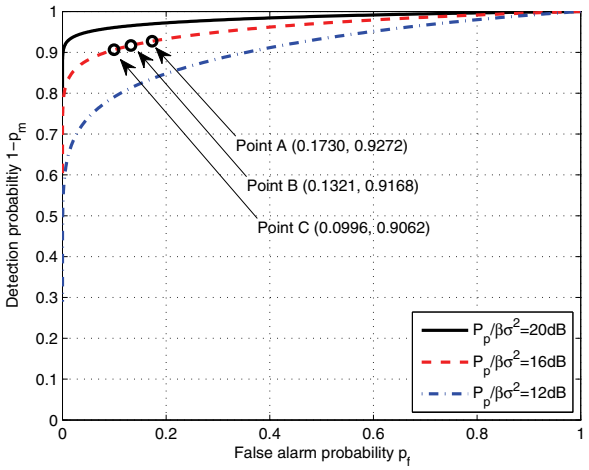

Fig. 3. ROC curves of the energy detector [6].

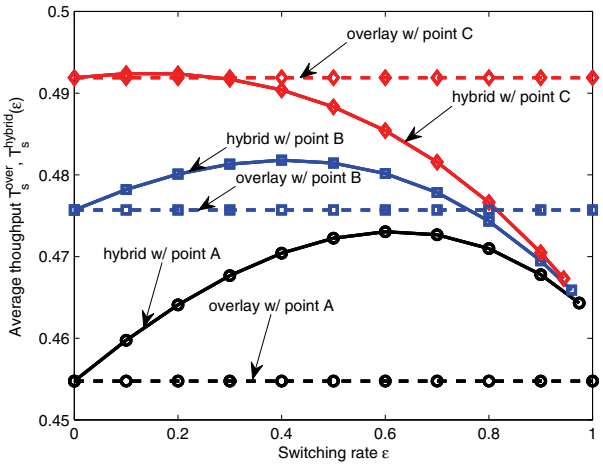

Fig. 4. Average throughput of the secondary user versus switching rate for different operation points in Fig.3.

greater than or equal to that of the overlay scheme. On the other hand, the secondary throughput of the hybrid scheme with the un-optimized ϵ could be smaller than that of the conventional overlay scheme even though the hybrid scheme provides more opportunity to access the spectrum. The reason why the secondary throughput of the hybrid scheme with un-optimized ϵ is smaller than that of the overlay scheme comes from the recursive interaction between the primary and secondary users. Although the interference to the primary user is regulated by underlay mode, the underlay transmission would interfere with the primary user and hence decreases $\mu_p^{hybrid}(\epsilon)$. If the transmission of the primary user fails due to the interference from the secondary user, the primary user tries to compensate for the degradation by retransmission (i.e., increasing $\frac{\lambda_p}{\mu_p^{hybrid}(\epsilon)}$). Then, that reaction of the primary user again affects the communication of the secondary user. In other words, as the value of ϵ increases, the primary user occupies the spectrum longer and the secondary user loses opportunity to access the spectrum without interference from the primary user. Eventually, in some environments where such losses of using underlay mode is greater than the gain of that, the throughput of the hybrid scheme with un-optimized ϵ could be worse than that of the overlay scheme. Of course, throughput of the hybrid scheme with optimized ϵ is always greater than or equal to that of the overlay scheme.

Fig. 5 shows ϵ_{opt} and ϵ_{max} according to the arrival rate of the primary user λ_p for different operation points in Fig. 3. Other system parameters are the same as those of Fig. 4. It is confirmed that ϵ_{max} decreases as the detection probability $1 - p_m$ increases and is not dependent on λ_p because the primary packet arrivals are not directly related to the successful transmission and the QoS constraint of the primary user. It is also confirmed that ϵ_{opt} decreases as λ_p increases beyond a certain value. This is because ϵ^* in (28) is a decreasing function of λ_p and it is clipped off if $\epsilon^* > \epsilon_{max}$. Because the secondary user becomes more likely to miss the opportunities to access the spectrum in overlay CR mode as p_f increases, a larger value of p_f increases the optimal switching rate ϵ_{opt}. In other words, as p_f increases, ϵ_{opt} also increases to recover the loss caused by the false alarm event.

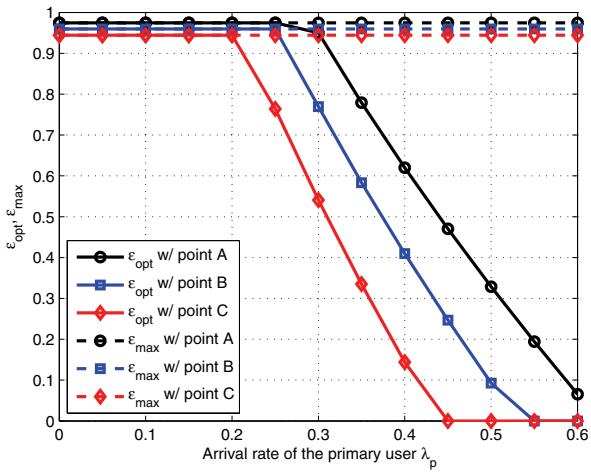

Fig. 5. Optimal and maximum switching rate versus arrival rate of the primary user for different operation points in Fig. 3.

Fig. 6 shows the secondary user's average throughputs in the overlay CR, underlay CR, and hybrid CR versus the arrival rate of the primary user λ_p for different operation points in Fig. 3. The optimal switching rates ϵ_{opt} in Fig. 5 are used in the hybrid CR system. Other system parameters are the same as those of Fig. 4. A larger value of λ_p implies the more frequent transmissions of the primary user (with probability λ_p/μ_p). That is, the probability that the secondary user loses the opportunity of spectrum access or receives interference from the primary user increases as λ_p grows. Therefore, growing λ_p reduces the departure rate of the secondary user no matter which CR mode is used. It is confirmed that the hybrid CR system has higher departure rate/average throughput than the conventional overlay and the conventional underlay CR systems. Furthermore, while T_s^{over} is greatly influenced by the sensing performance, $T_s^{hybrid}(\epsilon_{opt})$ is hardly affected.

To see the sensitivity of the throughput to p_f precisely, Fig. 7 shows the secondary throughputs in the overlay and hybrid CR systems versus the false alarm probability p_f for $p_m = 0.1$. Note that p_f and p_m in this figure does not come from one ROC curve, but comes from different ROC curves

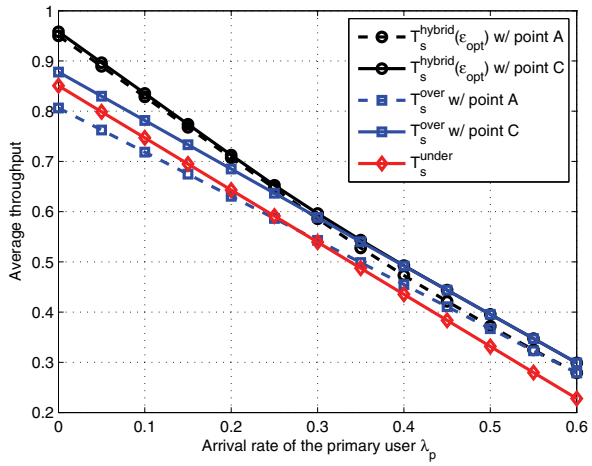

Fig. 6. Average throughput of the secondary user versus arrival rate of the primary user λ_p for different operation points in Fig. 3.

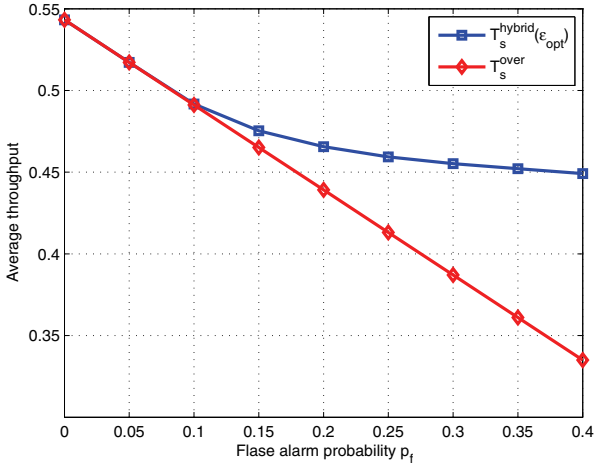

Fig. 7. Average throughput versus false alarm probability p_f for fixed miss detection probability p_m=0.1.

(i.e., As shown in Fig. 3, if average SNR $\frac{P_p}{\beta\sigma^2}$ changes, the detector has different ROC curves). In this simulation, τ is chosen to make a target missed detection probability p_m be equal to 0.1 with varying β and $\frac{P_p}{\sigma^2} = 16$[dB]. Other system parameters are selected the same as those of Fig. 4. It is shown that the secondary throughput of the hybrid CR is more robust to p_f than that of the conventional overlay CR. While p_f changes from 0.05 to 0.4, the loss of $T_s^{hybrid}(\epsilon_{opt})$ is only 17.3%, but that of T_s^{over} is 38.3%.

Fig. 8 shows the throughputs of the secondary user in the conventional CR schemes and the proposed hybrid CR scheme and the idle probability of the primary user in the hybrid CR scheme versus the transmit SNR of the primary user $\frac{P_p}{\sigma^2}$. The detection threshold τ is chosen to be 14, and other system parameters are the same as those of Fig. 4. It is interesting to note that the throughputs of the secondary user increase as the transmit SNR of the primary user grows. The increase in the transmit SNR of the primary user $\frac{P_p}{\sigma^2}$ improves not only the sensing performance at the secondary transmitter but also the received SINR at the primary receiver. The idle probability of the primary user $1 - \frac{\lambda_p}{\mu_p^{over}}$ increases owing to the improved received SINR at the primary receiver. In addition to the increased opportunity to access the spectrum, the improved sensing performance owing to high primary transmit power enables the secondary user in the overlay CR to more efficiently utilize the vacant spectrum without interfering the primary user. This indicates that the average throughput of the secondary user in overlay CR increases as the primary transmit power grows. On the other hand, although higher transmit power of the primary user degrades the received SINR of the secondary user in the underlay CR scheme when the primary user is busy, the busy probability of the primary user $\frac{\lambda_p}{\mu_p^{under}}$ is decreased by higher transmit power because the improved SINR at the primary receiver increases the departure rate μ_p^{under}. If the arrival rate λ_p is low, the gain obtained from higher primary transmit power is greater than the loss caused by higher primary transmit power. Because CR systems inherently assumes a low primary user activity, the average throughput of the secondary user in the underlay CR increases as primary transmit power grows. For the same reasons as the conventional CR schemes, the idle probability $p_i^{hybrid}(\epsilon_{opt}) = 1 - \frac{\lambda_p}{\mu_p^{hybrid}(\epsilon_{opt})}$ and the average throughput $T_s^{hybrid}(\epsilon_{opt})$ in hybrid CR scheme increases as the transmit SNR $\frac{P_p}{\sigma^2}$ grows. It is also shown that the throughput of the hybrid CR scheme coincides with that of the underlay CR scheme at the high primary transmit SNR $\frac{P_p}{\sigma^2}$; on the other hand, it coincides with the throughput of the overlay CR scheme at the low primary transmit SNR $\frac{P_p}{\sigma^2}$. When $\frac{P_p}{\sigma^2}$ is high enough, even if the secondary user uses its maximum power while the primary user is busy, the interference to the primary receiver cannot significantly degrade the departure rate of the primary user. It implies that operating like the secondary user in the underlay CR ($\epsilon_{opt} = 1$) with its maximum power $P_{s,max}$ is the optimal way to maximize the secondary throughput. On the other hand, when $\frac{P_p}{\sigma^2}$ is low, the primary departure rate is significantly degraded by the interference from the secondary user. In other words, avoiding interfering with the primary user is more important than concurrent transmission with the primary user to ensure the QoS constraint of the primary user. Consequently, operating like the secondary user in the overlay CR ($\epsilon_{opt} = 0$) is the optimal way to maximize the secondary throughput if $\frac{P_p}{\sigma^2}$ is low.

Fig. 9 shows secondary user's average throughputs of the hybrid CR scheme versus $\frac{P_{s,max}}{\sigma^2}$ for operation point A in Fig. 3. Other system parameters are the same as those of Fig. 4. The gap between the two curves is originated from the ability to adapt the transmit power to the interfering channel condition $|h_{sp}|^2$. It is shown that the gap becomes wider as the maximum transmit power $P_{s,max}$ grows because the higher $P_{s,max}$ enables the secondary transmitter with channel information of $|h_{sp}|^2$ to control power within the wider range.

Fig. 10 shows secondary user's average throughputs in the overlay, underlay, and hybrid CR schemes versus the number of the secondary user N. The overlay and hybrid CR schemes operate at point A in Fig. 3, and system parameters are the same as those of Fig. 4. It is confirmed that $T_s^{hybrid}(\epsilon_{opt})$ is almost the same as T_s^{under} and is greater than T_s^{over} when N is large. As the number of secondary user N increases,

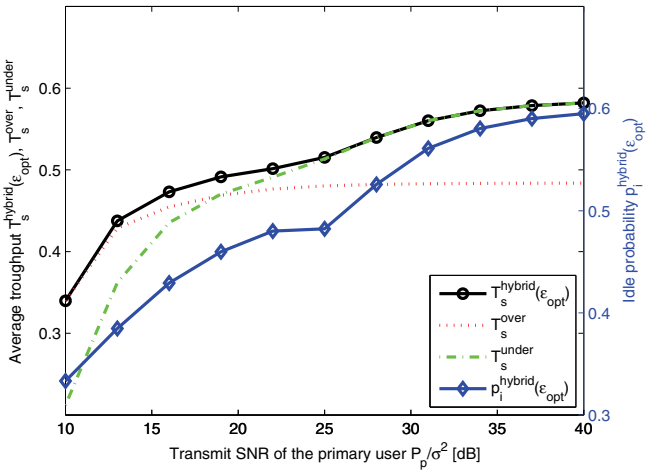

Fig. 8. Average throughput and idle probability of the primary user versus the transmit SNR of the primary user.

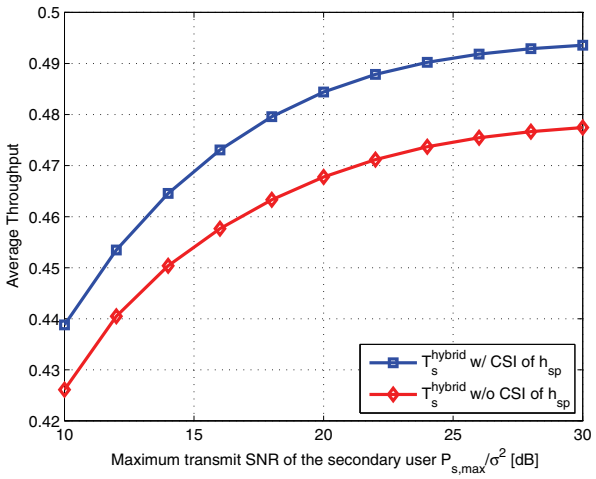

Fig. 9. Average throughput of the secondary user versus maximum transmit SNR.

both D^{over} and D^{under} converge to 1. This implies that the primary user is hardly affected by the secondary user in both the overlay and underlay CR schemes, and the secondary user transmits its data at anytime with underlay CR is more suitable than opportunistically with the overlay CR. Consequently, for large N, the optimal switching rate of hybrid CR approaches to 1 and the secondary user behaves like the secondary user in the underlay CR scheme.

VII. Conclusion

We showed that if the recursive interactions between the primary and secondary users are considered, the existing hybrid CR approaches which enable the secondary user to transmit all the time cannot always guarantee secondary user's improvement over conventional overlay CR systems. Motivated by this observation, we developed and analyzed a hybrid CR system that probabilistically switches the spectrum access modes between overlay and underlay CR modes for an increase of secondary user's throughput. The switching rate ϵ_{opt} was optimized to maximize secondary user's throughput while guaranteeing the QoS of the primary user. Our simulation

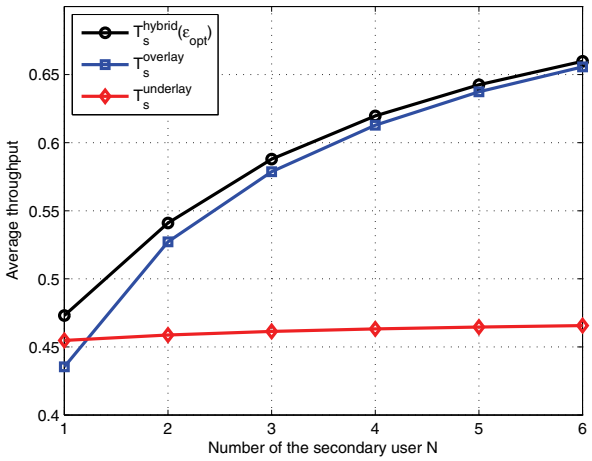

Fig. 10. Average throughput of the secondary user versus the number of the secondary user.

results confirmed that the hybrid CR system with optimized ϵ results in secondary user's throughput improvement over conventional CR systems. It was also shown that the hybrid CR is more robust to the sensing errors (i.e., the false alarm probability p_f) than conventional CR systems. Finally, we extended our work to the multiple secondary users scenarios in which one secondary user with the lowest interference channel power gain is scheduled for transmission.

Appendix A
Derivation of μ_p^{over}

The departure rate of the primary user in overlay CR μ_p^{over} can be represented as

$$\mu_p^{over} = (1-p_m)\Pr\left[\frac{|h_{pp}|^2 P_p}{\sigma^2} \geq a_p\right] + p_m \Pr\left[\frac{|h_{pp}|^2 P_p}{\sigma^2 + |h_{sp}|^2 P_s^{over}} \geq a_p\right]. \quad (34)$$

As shown in (34), the departure rate μ_p^{over} is composed of two terms. The first term represents the departure rate when the secondary user correctly detects the primary user's activity with the probability of $1-p_m$. In this case, the secondary user does not interfere with the primary user. The second term represents the departure rate when the secondary user misses detection of primary user's transmission. Note that the secondary user interferes with the successful communication of the primary user when it misses to detect the primary user. From (34), we can obtain μ_p^{over} as

$$\mu_p^{over} = (1-p_m)\exp\left(-\frac{\beta_{pp}a_p\sigma^2}{P_p}\right) + p_m \exp\left(-\frac{\beta_{pp}a_p\sigma^2}{P_p}\right)\left(\frac{\beta_{sp}P_p}{\beta_{sp}P_p + \beta_{pp}a_p P_s^{over}}\right). \quad (35)$$

Appendix B
Derivation of μ_s^{over}

Since the secondary user in overlay CR uses the spectrum only when it is detected as an idle state, the departure rate of the secondary user heavily depends on the probability that

primary user is idle. By queuing theory, the idle probability of the primary user, or the probability that the primary user's queue is empty, is represented as $1-\frac{\lambda_p}{\mu_p^{over}}$. Therefore, the departure rate of the secondary user in the overlay CR μ_s^{over} can be represented as

$$\mu_s^{over}=\left(1-\frac{\lambda_p}{\mu_p^{over}}\right)(1-p_f)\mu_{s,idle}^{over}+\frac{\lambda_p}{\mu_p^{over}}p_m\mu_{s,active}^{over}, \quad (36)$$

where $\mu_{s,idle}^{over}$ and $\mu_{s,active}^{over}$ denote the departure rates when the secondary user correctly detects the absence of primary user's transmission and when the secondary user misses primary user's transmission, respectively. Hence, $\mu_{s,idle}^{over}$ and $\mu_{s,active}^{over}$ can be represented as

$$\mu_{s,idle}^{over}=\Pr\left[\frac{|h_{ss}|^2P_s^{over}}{\sigma^2}\geq a_s\right]=\exp\left(-\frac{\beta_{ss}a_s\sigma^2}{P_s^{over}}\right), \quad (37)$$

$$\begin{aligned}\mu_{s,active}^{over}&=\Pr\left[\frac{|h_{ss}|^2P_s^{over}}{\sigma^2+|h_{ps}|^2P_p}\geq a_s\right]\\&=\exp\left(-\frac{\beta_{ss}a_s\sigma^2}{P_s^{over}}\right)\left(\frac{\beta_{ps}P_s^{over}}{\beta_{ps}P_s^{over}+\beta_{ss}a_sP_p}\right), \quad (38)\end{aligned}$$

respectively, where $a_s=2^{R_s}-1$.

Appendix C
Derivation of μ_p^{under}

Based on (10), the departure rate of the primary user in underlay CR μ_p^{under} is composed of two terms.

$$\begin{aligned}\mu_p^{under}&=\Pr\left[|h_{sp}|^2\leq\frac{Q}{P_{s,max}},\frac{|h_{pp}|^2P_p}{\sigma^2+|h_{sp}|^2P_{s,max}}\geq a_p\right]\\&+\Pr\left[|h_{sp}|^2>\frac{Q}{P_{s,max}},\frac{|h_{pp}|^2P_p}{\sigma^2+|h_{sp}|^2\frac{Q}{|h_{sp}|^2}}\geq a_p\right], \quad (39)\end{aligned}$$

where $\Pr[A,B]$ represents the probability of event A and event B. Hence, μ_p^{under} is obtained as

$$\begin{aligned}\mu_p^{under}&=\exp\left(-\frac{\beta_{pp}a_p\sigma^2}{P_p}\right)\frac{\beta_{sp}P_p}{\beta_{sp}P_p+\beta_{pp}a_pP_{s,max}}\\&+\frac{\exp\left(-\frac{\beta_{pp}a_p\sigma^2}{P_p}-\frac{(\beta_{pp}a_pP_{s,max}+\beta_{sp}P_p)Q}{P_pP_{s,max}}\right)\beta_{pp}a_p}{\frac{\beta_{sp}P_p}{P_{s,max}}+\beta_{pp}a_p}. \quad (40)\end{aligned}$$

Appendix D
Derivation of μ_s^{under}

The departure rate of the secondary user in underlay CR μ_s^{under} is written by

$$\mu_s^{under}=\left(1-\frac{\lambda_p}{\mu_p^{under}}\right)\mu_{s,idle}^{under}+\frac{\lambda_p}{\mu_p^{under}}\mu_{s,active}^{under}, \quad (41)$$

where $\mu_{s,idle}^{under}$ and $\mu_{s,active}^{under}$ are the departure rates of secondary user when the primary user is idle and when the primary user is active, respectively. Hence, they can be represented respectively by

$$\mu_{s,idle}^{under}=\Pr\left[\frac{|h_{ss}|^2P_s^{under}}{\sigma^2}\geq a_s\right], \quad (42)$$

$$\mu_{s,active}^{under}=\Pr\left[\frac{|h_{ss}|^2P_s^{under}}{\sigma^2+|h_{ps}|^2P_p}\geq a_s\right]. \quad (43)$$

Derivations of $\mu_{s,idle}^{under}$ and $\mu_{s,active}^{under}$ are following. Based on (10), the departure rate $\mu_{s,idle}^{under}$ is composed of two terms

$$\begin{aligned}\mu_{s,idle}^{under}&=\Pr\left[|h_{sp}|^2\leq\frac{Q}{P_{s,max}},\frac{|h_{ss}|^2P_{s,max}}{\sigma^2}\geq a_s\right]\\&+\Pr\left[|h_{sp}|^2>\frac{Q}{P_{s,max}},\frac{|h_{ss}|^2\frac{Q}{|h_{sp}|^2}}{\sigma^2}\geq a_s\right]. \quad (44)\end{aligned}$$

The first term in (44) is easily solved. In the second term, let $X=|h_{ss}|^2$, $Y=|h_{sp}|^2$, and $Z=\frac{XQ}{Y\sigma^2}$. Since X and Y are exponential random variables, the joint PDF of Y and Z can be represented as

$$\begin{aligned}f_{Z,Y}(z,y)&=f_{Z|Y}(z|y)f_Y(y)\\&=\beta_{ss}\frac{y\sigma^2}{Q}\exp\left(-\beta_{ss}\frac{y\sigma^2}{Q}z\right)\beta_{sp}\exp\left(-\beta_{sp}y\right). \quad (45)\end{aligned}$$

Then, the second term in (44) can be calculated by

$$\begin{aligned}&\Pr\left[|h_{sp}|^2>\frac{Q}{P_{s,max}},\ \frac{|h_{ss}|^2\frac{Q}{|h_{sp}|^2}}{\sigma^2}\geq a_s\right]\\&=\int_{\frac{Q}{P_{s,max}}}^{\infty}\int_{a_s}^{\infty}f_{Z,Y}(z,y)dzdy\\&=\frac{\beta_{ss}Q}{\beta_{ss}a_s\sigma^2+\beta_{sp}Q}\exp\left(-\frac{\beta_{ss}a_s\sigma^2+\beta_{sp}Q}{P_{s,max}}\right). \quad (46)\end{aligned}$$

Consequently, the departure rate $\mu_{s,idle}^{under}$ is represented as

$$\begin{aligned}\mu_{s,idle}^{under}&=\left(1-\exp\left(-\frac{\beta_{sp}Q}{P_{s,max}}\right)\right)\exp\left(-\frac{\beta_{ss}a_s\sigma^2}{P_{s,max}}\right)\\&+\frac{\beta_{sp}Q\exp\left(-\frac{\beta_{ss}a_s\sigma^2+\beta_{sp}Q}{P_{s,max}}\right)}{\beta_{ss}a_s\sigma^2+\beta_{sp}Q}. \quad (47)\end{aligned}$$

Now, let's derive $\mu_{s,active}^{under}$. Based on (10), the departure rate $\mu_{s,active}^{under}$ is composed of two terms

$$\begin{aligned}\mu_{s,active}^{under}&=\Pr\left[|h_{sp}|^2\leq\frac{Q}{P_{s,max}},\frac{|h_{ss}|^2P_{s,max}}{\sigma^2+|h_{ps}|^2P_p}\geq a_s\right]\\&+\Pr\left[|h_{sp}|^2>\frac{Q}{P_{s,max}},\frac{|h_{ss}|^2\frac{Q}{|h_{sp}|^2}}{\sigma^2+|h_{ps}|^2P_p}\geq a_s\right]. \quad (48)\end{aligned}$$

The first term in (48) is easily solved. In the second term, let $X=|h_{ss}|^2$, $Y=|h_{ps}|^2$, and $Z=\frac{XQ}{\sigma^2+YP_p}$. Since X and Y are exponential random variables, the joint PDF of Y and Z and the PDF of Z are obtained, respectively, as

$$\begin{aligned}f_{Z,Y}(z,y)&=f_{Z|Y}(z|y)f_Y(y)\\&=\frac{\beta_{ps}\beta_{ss}(\sigma^2+yP_p)\exp\left(-\frac{\beta_{ss}(\sigma^2+yP_p)z}{Q}-\beta_{ps}y\right)}{Q}, \quad (49)\\f_Z(z)&=\int_0^{\infty}f_{Z,Y}(z,y)dy\\&=\frac{\beta_{ps}\beta_{ss}(\beta_{ps}Q\sigma^2+QP_p+\beta_{ss}P_p\sigma^2z)\exp\left(\frac{-\beta_{ss}\sigma^2z}{Q}\right)}{(\beta_{ss}P_pz+\beta_{ps}Q)^2}. \quad (50)\end{aligned}$$

Let V=$|h_{sp}|^2$, $W = \frac{Z}{V}$, and the joint PDF of V and W is

$$\begin{aligned} f_{W,V}(w,v) &= f_{W|V}(w|v) f_V(v) \\ &= v\beta_{ss}\beta_{ps} \exp\left(-\frac{\beta_{ss}\sigma^2 vw}{Q}\right) \\ &\quad \times \frac{\beta_{ps}Q\sigma^2 + QP_p + \beta_{ss}P_p\sigma^2 vw}{\left(\beta_{ss}P_p vw + \beta_{ps}Q\right)^2} \beta_{sp} \exp\left(-\beta_{sp}v\right). \end{aligned} \quad (51)$$

Accordingly, the second term in (48) is obtained by

$$\begin{aligned} &\Pr\left[|h_{sp}|^2 > \frac{Q}{P_{s,max}}, \frac{|h_{ss}|^2 \frac{Q}{|h_{sp}|^2}}{\sigma^2 + |h_{ps}|^2 P_p} \geq a_s\right] \\ &= \int_{\frac{Q}{P_{s,max}}}^{\infty} \int_{a_s}^{\infty} f_{W,V}(w,v) dw dv \\ &= \frac{\beta_{sp}\beta_{ps}Q}{\beta_{ss}a_s P_p} \exp\left(\frac{\beta_{ps}(\beta_{ss}a_s\sigma^2 + \beta_{sp}Q)}{\beta_{ss}a_s P_p}\right) \\ &\quad \times E_1\left(\frac{(\beta_{ss}a_s P_p + \beta_{ps}P_{s,max})(\beta_{ss}a_s\sigma^2 + \beta_{sp}Q)}{\beta_{ss}a_s P_p P_{s,max}}\right), \end{aligned} \quad (52)$$

where $E_1(x) = \int_x^{\infty} \frac{\exp(-u)}{u} du$.

Consequently, the departure rate $\mu_{s,active}^{under}$ is obtained by

$$\begin{aligned} \mu_{s,active}^{under} &= \left(1 - \exp\left(-\frac{\beta_{sp}Q}{P_{s,max}}\right)\right) \exp\left(-\frac{\beta_{ss}a_s\sigma^2}{P_{s,max}}\right) \\ &\quad \times \left(\frac{\beta_{ps}P_{s,max}}{\beta_{ps}P_{s,max} + \beta_{ss}a_s P_p}\right) \\ &\quad + E_1\left(\frac{(\beta_{ss}a_s P_p + \beta_{ps}P_{s,max})(\beta_{ss}a_s\sigma^2 + \beta_{sp}Q)}{\beta_{ss}a_s P_p P_{s,max}}\right) \\ &\quad \times \frac{\beta_{sp}\beta_{ps}Q}{\beta_{ss}a_s P_p} \exp\left(\frac{\beta_{ps}(\beta_{ss}a_s\sigma^2 + \beta_{sp}Q)}{\beta_{ss}a_s P_p}\right). \end{aligned} \quad (53)$$

APPENDIX E
UNDERLY CR WITHOUT CHANNEL STATE INFORMATION OF THE INTERFERING LINK

The transmit power of the secondary user in the underlay CR without the interfering channel information is denoted by $\bar{P}_s^{under}$. In this case, the secondary user transmits a packet with a fixed power, and the power $\bar{P}_s^{under}$ can be determined to satisfy the QoS constraint of the primary as below

$$\bar{\mu}_p^{under} = \Pr\left[\frac{|h_{pp}|^2 P_p}{\sigma^2 + |h_{sp}|^2 \bar{P}_s^{under}} > a_p\right] \geq \mu_{th}. \quad (54)$$

Using the distributions of $|h_{pp}|^2$ and $|h_{sp}|^2$, we can obtain the maximum allowable power to guarantee the QoS constraint $\bar{P}_{s,\mu}^{under}$ from (54) by

$$\bar{P}_{s,\mu}^{under} = \frac{\beta_{sp}P_p}{\beta_{pp}a_p}\left[\frac{1}{\mu_{th}\exp(\frac{\beta_{pp}a_p\sigma^2}{P_p})} - 1\right] = \frac{\bar{Q}}{\mathbb{E}[|h_{sp}|^2]}, \quad (55)$$

where $\bar{Q} = \frac{P_p}{\beta_{pp}a_p}\left[\frac{1}{\mu_{th}\exp(\frac{\beta_{pp}a_p\sigma^2}{P_p})} - 1\right]$ denotes the interference temperature when the secondary user does not have the instantaneous channel information of $|h_{sp}|^2$. If the channel power gain of h_{sp} has the mean $\mathbb{E}[|h_{sp}|^2] = 1$, the maximum allowable power of the secondary user is the same as the interference temperature $\bar{Q}$. Based on (55), the actual transmit power of the secondary user $\bar{P}_s^{under}$ is determined by

$$\bar{P}_s^{under} = \begin{cases} P_{s,max}, & \text{if } P_{s,max} \leq \frac{\bar{Q}}{\mathbb{E}[|h_{sp}|^2]} \\ \bar{P}_{s,\mu}^{under} = \frac{\bar{Q}}{\mathbb{E}[|h_{sp}|^2]}, & \text{if } P_{s,max} > \frac{\bar{Q}}{\mathbb{E}[|h_{sp}|^2]} \end{cases}. \quad (56)$$

Then, the departure rate of the primary user $\bar{\mu}_p^{under}$ can be written as

$$\begin{aligned} \bar{\mu}_p^{under} &= \mathbf{1}\left(P_{s,max} \leq \frac{\bar{Q}}{\mathbb{E}[|h_{sp}|^2]}\right)\left(\frac{\beta_{sp}P_p}{\beta_{sp}P_p + \beta_{pp}a_p P_{s,max}}\right) \\ &\quad + \mathbf{1}\left(P_{s,max} > \frac{\bar{Q}}{\mathbb{E}[|h_{sp}|^2]}\right)\left(\frac{P_p}{P_p + \beta_{pp}a_p\bar{Q}}\right), \end{aligned} \quad (57)$$

where $\mathbf{1}(\cdot)$ is the indicator function; if event X is true, $\mathbf{1}(X) = 1$ and otherwise, $\mathbf{1}(X) = 0$. Then, The throughput of the primary user is represented by $\bar{T}_p^{under} = R_p\bar{\mu}_p^{under}$.

The departure rate of the secondary user $\bar{\mu}_s^{under}$ is represented as

$$\bar{\mu}_s^{under} = \left(1 - \frac{\lambda_p}{\bar{\mu}_p^{under}}\right)\bar{\mu}_{s,idle}^{under} + \frac{\lambda_p}{\bar{\mu}_p^{under}}\bar{\mu}_{s,active}^{under}, \quad (58)$$

where $\bar{\mu}_{s,idle}^{under}$ and $\bar{\mu}_{s,active}^{under}$ are defined by

$$\begin{aligned} \bar{\mu}_{s,idle}^{under} &= \Pr\left[\frac{|h_{ss}|^2 \bar{P}_s^{under}}{\sigma^2} \geq a_s\right] \\ &= \mathbf{1}\left(P_{s,max} \leq \frac{\bar{Q}}{\mathbb{E}[|h_{sp}|^2]}\right)\exp\left(-\frac{\beta_{ss}a_s\sigma^2}{P_{s,max}}\right) \\ &\quad + \mathbf{1}\left(P_{s,max} > \frac{\bar{Q}}{\mathbb{E}[|h_{sp}|^2]}\right)\exp\left(-\frac{\beta_{ss}a_s\sigma^2}{\bar{Q}/\mathbb{E}[|h_{sp}|^2]}\right), \end{aligned} \quad (59)$$

$$\begin{aligned} \bar{\mu}_{s,active}^{under} &= \Pr\left[\frac{|h_{ss}|^2 P_s^{under,avg}}{\sigma^2 + |h_{ps}|^2 P_p} \geq a_s\right] \\ &= \mathbf{1}\left(P_{s,max} \leq \frac{\bar{Q}}{\mathbb{E}[|h_{sp}|^2]}\right)\left(\frac{\beta_{ps}P_{s,max}\exp\left(-\frac{\beta_{ss}a_s\sigma^2}{P_{s,max}}\right)}{\beta_{ps}P_{s,max} + \beta_{ss}a_s P_p}\right) \\ &\quad + \mathbf{1}\left(P_{s,max} > \frac{\bar{Q}}{\mathbb{E}[|h_{sp}|^2]}\right)\left(\frac{\beta_{ps}\bar{Q}\exp\left(\frac{-\beta_{ss}a_s\sigma^2}{\bar{Q}/\mathbb{E}[|h_{sp}|^2]}\right)}{\beta_{ps}\bar{Q} + \mathbb{E}[|h_{sp}|^2]\beta_{ss}a_s P_p}\right). \end{aligned} \quad (60)$$

The throughput of the secondary user in underlay CR is represented by $\bar{T}_s^{under} = R_s\bar{\mu}_s^{under}$.

APPENDIX F
PROOF OF COROLLARY 1

As $N \to \infty$, the optimization problem (18) are simplified by $\epsilon_{max} = 1$ and $E = 0$. Consequently, the optimization problem (18) is rewritten as

$$\max_{0 \leq \epsilon \leq 1} \left(A + \frac{C}{D}\right)\epsilon + \frac{B}{D}. \quad (61)$$

Furthermore, as $N \to \infty$, we get

$$\mu_{s,idle}^{under} = \mu_{s,idle}^{over} = \exp\left(-\frac{\beta_{ss,\hat{i}}a_s\sigma^2}{P_{s,max}}\right), \quad (62)$$

$$\mu_{s,active}^{under} = \mu_{s,active}^{over} = \frac{\exp\left(-\frac{\beta_{ss,\hat{i}}a_s\sigma^2}{P_{s,max}}\right)\beta_{ps}P_{s,max}}{\beta_{ps}P_{s,max} + \beta_{ss,\hat{i}}a_s P_p}, \quad (63)$$

where $\mathbb{E}\left[|h_{ss,\hat{i}}|^2\right] = 1/\beta_{ss,\hat{i}}$, and $h_{ss,\hat{i}}$ is the channel gain between the selected secondary transmitter and the secondary receiver. According to (62) and (63), $\left(A + \frac{C}{D}\right) > 0$; therefore, the secondary throughput is maximized at the switching rate $\hat{\epsilon}_{opt} = 1$. Because the secondary transmit powers of both conventional CR schemes converge to $P_{s,max}$ for a large N, the hybrid CR scheme with $\hat{\epsilon}_{opt}$ behaves like the conventional underlay CR scheme with opportunistically selected secondary user. Therefore, if the number of the secondary user N is large, the throughput of the hybrid CR scheme is equivalent to that of the conventional underlay CR scheme with opportunistically selected secondary user; $T_s^{hybrid}(\epsilon_{opt}) = T_s^{under}$.

REFERENCES

[1] Federal Communications Commission, Spectrum Policy Task Force Report, ETDocket No.02-135, Nov. 2002.

[2] J. Mitola and G. Q. Maguire, "Cognitive radios: making software radios more personal," *IEEE Personal Commun.*, vol. 6, no. 4, pp. 1318, Aug. 1999.

[3] Q. Zhao and B. M. Sadler, "A survey of dynamic spectrum access," *IEEE Signal Process. Mag.*, vol. 24, no. 3, pp. 79–89, May 2007.

[4] D. Cabric, S. M. Mishra, and R. W. Brodersen, "Implementation issues in spectrum sensing for cognitive radios," in *Proc. 2004 Asilomar Conf. Signals, Syst. Comput.*

[5] W. Gardner, "Signal interception: a unifying theoretical framework for feature detection," *IEEE Trans. Commun.,* vol. 36, pp. 897–906, Aug. 1988.

[6] A. Ghasemi and E. S. Sousa, "Collaborative spectrum sensing for opportunistic access in fading environment," in *Proc. 2005 IEEE Int'l Symp. Dynamic Spectrum Access Netw.*

[7] Y. C. Liang, Y. Zeng, E. C. Y. Peh, and A. T. Hoang, "Sensing throughput tradeoff for cognitive radio networks," *IEEE Trans. Wireless Commun.*, vol. 7, no. 4, pp. 1326–1337, Apr. 2008.

[8] O. Simeone, Y. Bar-Ness, and U. Spagnolini, "Stable throughput of cognitive radios with and without relaying capability," *IEEE Trans. Commun.*, vol. 55, no. 12, pp. 2351–2360, Dec. 2007.

[9] J. Gambini, O. Simeone, Y. Bar-Ness, U. Spagnolini, and T. Yu, "Packet-wise vertical handover for unlicensed multi-standard spectrum access with cognitive radios," *IEEE Trans. Wireless Commun.*, vol. 7, no. 12, pp. 5172–5176, Dec. 2008.

[10] J. P. Hong and W. Choi, "Throughput characteristics by multiusr diversity in a cognitive radio system," *IEEE Trans. Signal Process.*, vol. 59, no. 8, pp. 3749–3763, Aug. 2011.

[11] S. Haykin, "Cognitive radio: brain-empowered wireless communications," *IEEE J. Sel. Areas Commun.*, vol. 23, no. 2, pp. 201–220, Feb. 2005.

[12] H. Arslan and M. Sahin, "UWB-based cognitive radio networks," *Cognitive Radio, Software Defined Radio and Adaptive Wireless Systems*. Springer, 2007.

[13] A. Ghasemi and E. S. Sousa, "Fundamental limits of spectrum sharing in fading environments," *IEEE Trans. Wireless Commun.*, vol. 6, no. 2, pp. 649–658, Feb. 2007.

[14] X. Kang, Y. C. Liang, A. Nallanathan, H. K. Garg, and R. Zhang, "Optimal power allocation for fading channels in cognitive radio networks: Ergodic capacity and outage capacity," *IEEE Trans. Wireless Commun.*, vol. 8, no. 2, pp. 940–950, Feb. 2009.

[15] T. W. Ban, W. Choi, B. C. Jung, and D. K. Sung, "Multi-user diversity in a spectrum sharing system," *IEEE Trans. Wireless Commun.*, vol. 8, no. 1, pp. 102–106, Jan. 2009.

[16] R. Zhang, S. Cui, and Y. C. Liang, "On ergodic sum capacity of fading cogntive multiple-access and broadcast channels," *IEEE Trans. Inf. Theory*, vol. 55, no. 11, pp. 5161–5178, May 2009.

[17] J.-P Hong, B. Hong, T. W. Ban, and W. Choi, "On the cooperative divresity gain in underlay cognitive radio systems," *IEEE Trans. Commun.*, vol. 60, no. 1, pp. 209–219, Jan. 2012.

[18] V. Chakravarthy, X. Li, Z. Wu, M. Temple, F. Garber, and R. Kannan, "Novel overlay/underlay cognitive radio waveforms using SD-SMSE framework to enhance spectrum efficiency—part I: theoretical framework and analysis in AWGN channel," *IEEE Trans. Commun.*, vol. 57, no. 12, pp. 3794–3804, Dec. 2009.

[19] V. Chakravarthy, X. Li, R. Zhou, Z. Wu, and M. Temple, "Novel overlay/underlay cognitive radio waveforms using SD-SMSE framework to enhance spectrum efficiency—part II: analysis in fading channels," *IEEE Trans. Commun.*, vol. 58, no. 6, pp. 1868–1876, June 2010.

[20] X. Kang, Y. C. Liang, H. K, Garg, and L. Zhang, "Sensing-based spectrum sharing in cognitive radio networks," *IEEE Trans. Veh. Technol.*, vol. 58, no. 8, pp. 4649–4654, Oct. 2009.

[21] S. Stotas and A. Nallanathan, "Enhancing the capacity of spectrum sharing cognitive radio networks," *IEEE Trans. Veh. Technol.*, vol. 60, no. 8, pp. 3768–3779, Oct. 2011.

[22] M. G. Khoshkholgh, K. Navaie, and H. Yanikomeroglu, "Access strategies for spectrum sharing in fading environment: overlay, underlay, and mixed," *IEEE Trans. Mobile Comput.*, vol. 9, no. 12, pp. 1780–1793, Dec. 2010.

[23] J. Oh and W. Choi, "A hybrid cognitive radio system: a combination of underlay and overlay approaches," in *Proc. 2010 IEEE VTC Conf. – Fall*.

[24] R. M. Loynes, "The stability of a queue with non-independent inter-arrival and service times," *Proc. Camb. Philos. Soc.*, vol. 58, pp. 497–520, July 1962.

[25] D. P. Bertsekas and J. N. Tsitsiklis, *Introduction to Probability*, 2nd edition. Athena Scientific, 2008.

Hojin Song (S'12) received the B.S. degree in electrical and computer engineering from University of Seoul (UOS), Seoul, Korea, in 2008. He is currently working toward the M.S. degree in electrical engineering from Korea Advance Institute of Science and Technology (KAIST), Daejeon, Korea. His research interests are cognitive radio and cooperative communication.

Jun-pyo Hong received the B.S. degree in electrical engineering from Information and Communications University (ICU), Daejeon, Korea, in 2008. In February 2010, he received the M.S. degree in electrical engineering from Korea Advance Institute of Science and Technology (KAIST), Daejeon, Korea. He is currently working towards the Ph.D. degree at Korea Advance Institute of Science and Technology (KAIST), Daejeon, Korea. His current research interests include cognitive radio, cooperative communication, and compressed sensing.

Wan Choi (S'03-M'06-SM12) received the B.Sc. and M.Sc. degrees from the School of Electrical Engineering and Computer Science (EECS), Seoul National University (SNU), Seoul, Korea, in 1996 and 1998, respectively, and the Ph.D. degree in the Department of Electrical and Computer Engineering at the University of Texas at Austin in 2006. He is currently an Associate Professor of the Department of Electrical Engineering, Korea Advance Institute of Science and Technology (KAIST), Daejeon, Korea. He was an Assistant Professor in the School of Engineering, Information and Communications University (ICU), Daejeon, Korea, from February 2007 to February 2009. From 1998 to 2003, he was a Senior Member of the Technical Staff of the R&D Division of KT Freetel Company, Limited, Korea, where he researched 3G CDMA systems. He also researched at Freescale Semiconductor and Intel Corporation during 2005 and 2006 summers, respectively, where he collaborated with them on practical wireless communication issues.

Dr. Choi is the recipient of IEEE Vehicular Technology Society Jack Neubauer Memorial Award which recognized the best paper published in the IEEE TRANSACTIONS ON VEHICULAR TECHNOLOGY for 2001. He also received the IEEE Vehicular Technology Society Dan Noble Fellowship Award in 2006 and the IEEE Communication Society Asia Pacific Young Researcher Award in 2007. While at the University of Texas at Austin, he was the recipient of William S. Livingston Graduate Fellowship and Information and Telecommunication Fellowship from Ministry of Information and Communication (MIC), Korea. He serves as Associate Editor for the IEEE TRANSACTIONS ON WIRELESS COMMUNICATIONS, for the IEEE TRANSACTIONS ON VEHICULAR TECHNOLOGY, and for the IEEE WIRELESS COMMUNICATIONS LETTERS. He was Co-Chair of the PHY track in the IEEE WCNC 2011 and the MIMO symposium in the IEEE IWCMC 2008. He was also a Publication Chair of IEEE WiOpt 2009.